# A DDA enhanced locally resonant metamaterial: experimental testing on a Lego® Technic assembly



**Author(s):**
Kalderon, Moris; Mantakas, Antonios; Chondrogiannis, Kyriakos Alexandros; Antoniadis, Ioannis A.

**Publication date:**
2023-06

**Permanent link:**
https://doi.org/https://doi.org/10.3929/ethz-b-000652218



**Originally published in:**
Journal of Physics: Conference Series 2647(17), https://doi.org/10.1088/1742-6596/2647/17/172001

**Funding acknowledgement:**
- INNOVATIVE GROUND INTERFACE CONCEPTS FOR STRUCTURE PROTECTION ()

Journal of Physics: Conference Series **2647** (2024) 172001 doi:10.1088/1742-6596/2647/17/172001

# A DDA enhanced locally resonant metamaterial: experimental testing on a Lego® Technic assembly

**M. Kalderon[1*], A. Mantakas[2], K.A. Chondrogiannis[3], I.A. Antoniadis[1]**

[1] National Technical University of Athens, School of Mechanical Engineering, Department of Mechanical Design & Automatic Control, Dynamics & Acoustics Laboratory Heroon Polytechniou 9, 15780 Zografou, Athens, Greece.

[2] National Technical University of Athens, School of Civil Engineering, Department of Structural Engineering, Institute of Structural Analysis and Antiseismic Research Heroon Polytechniou 9, 15780 Zografou, Athens, Greece.

[3] ETH Zurich, Department of Civil, Environmental and Geomatic Engineering Stefano-Franscini-Platz 5, Zurich 8093, Switzerland

[*]moriska@mail.ntua.gr

**Abstract**. Locally resonant metamaterials (LRMs), with periodic elements that exhibit local resonance, have been recently investigated by numerous researchers as a means to pursue vibration attenuation and wave manipulation. These structures are able to generate bandgaps in specific frequency ranges depending on their mass, stiffness and geometrical characteristics; however, they present certain limitations when bandgaps in the low-frequency domain are sought, since they require heavy oscillating masses. This research work harnesses the potency of a novel dynamic directional amplifier, namely the DDA, that is introduced as a means to artificially increase the inertia of an oscillating mass. The DDA is realized by imposing kinematic constraints to the degrees of freedom (DoFs) of the oscillator, hence inertia is increased by coupling the horizontal and vertical motion and forcing the model to move along a circumference. Herein, the DDA is applied on the resonating mass of a scaled LRM structure, assembled using LEGO® components. Experimental and analytical calculations are subsequently undertaken to investigate the dynamic properties of this DDA-enhanced metamaterial. Results showcase the low-frequency attenuation properties of the structure and serve as a proof of concept of the mechanism.

## 1. Introduction

The field of metamaterials has seen significant advancements in recent years, with the development of acoustic (AM) and locally resonant (LR) metamaterials showcasing exceptional dynamic properties. These materials rely on their unique microstructures to create a filtering effect, resulting in the formation of bandgaps. When an impacting excitation has a frequency that falls into the blind zone generated by the bandgap, the propagation of waves is blocked [1–3]. However, despite their potential for extraordinary dynamic properties, conventional LRMs [4] may face challenges in achieving wide

and low-frequency bandgaps due to the hefty internal parasitic masses and additional constraints, which can complicate their implementation [5]. To overcome these challenges, researchers have explored the use of inerters in both local resonating masses and the lattice structure of inertant acoustic metamaterials [5,6]. Analysis has shown that the bandgap range can be modified depending on the inerter configuration and properties with minimal mass addition to the metamaterial structure. Similarly, researchers have developed architected metamaterial structures with inertial amplification mechanisms [7–9] or negative stiffness [10] properties, and tested them experimentally. Several attempts have been made [11,12], including the exploration of chirality [13] and geometrically nonlinear metamaterials [14]. Recently, Kalderon et al. proposed a new class of enhanced metamaterials, including both phononic [15,16] and LR [17,18] structures, that utilize a dynamic directional amplification mechanism known as the DDA [19].
In this context, the use of dynamic directional amplification mechanisms (DDA) has been proposed as a way to enhance the performance of these materials. The paper at hand seeks to verify the benefits of incorporating DDA mechanisms within the structure by designing and testing inertial amplified locally resonant prototypes constructed using LEGO® technic bricks. Results from the experiments validate the concept of DDA-enhanced structures and demonstrate that the proposed metamaterials can be adequately described by analytical and numerical models. The established prototypes indicate that realistic full-scale designs are feasible and suitable for a wide range of applications, such as seismic mitigation, vibration isolation, and acoustic mitigation. These findings represent a significant step forward in the development of innovative materials with extraordinary dynamic properties.

## 2. Theoretical background

### *2.1. The Dynamic Directional Amplification (DDA) mechanism*

The Cartesian coordinate system is established as shown in Figure 1. Connecting the mass to the origin of the local coordinate system (CSYS) via a hinged, rigid rod of length AB=L which is assumed to be massless for the purpose of this analysis, imposes a kinematic constraint between the DoFs u and v. The lumped parameter model is described by the coordinates of the mass (m) at a generic position B($x$, $y$)=($x_0$+$u$, $y_0$−$v$), where $x_0$, $y_0$ are the initial coordinates of the mass. The initial angle between the horizontal axis and the link is denoted by $\varphi = arctan(x_0 / y_0)$, while $\theta$ denotes the rotation of the rod at the generic position B of the moving mass. $k_x$, $k_y$ are the springs stiffnesses, $c_x$, $c_y$ the damping coefficient on the horizontal and vertical directions respectively, and F the force exciting the mass in the x direction. The governing equation of the DDA mechanism in the direction of motion is given as follows:

$$M\ddot{u} + C\dot{u} + Ku = F \tag{1}$$

where, $M = (1 + tan^2(\varphi))m$, $C = c_x + c_y tan^2(\varphi)$ and $K = k_x + k_y tan^2(\varphi)$.

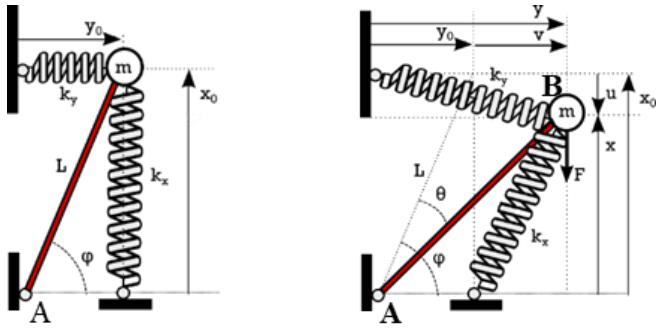


(a) (b)

**Figure 1.** Kinematic model of the Dynamic directional amplification (DDA) mechanism, where the motion of v mass m is kinematically constrained to the motion u, (a) initial mass position (b) mass position at deformed state.

*2.2. 2D phononic lattice with Dynamic Directional Amplification (DDA) mechanisms*

The effective lattice of a mass-in-mass setup, which includes an external mass ( $m_L$ ), an internal resonator ( $m_R$ ), and weightless springs and dashpots, is illustrated in Figure 2. Using this basic arrangement, the improved unit-cells are envisioned. Figure 2 (a) demonstrates the layout of a typical LR unit-cell, whereas (b) displays the unit-cell with the DDA attached to the resonating mass ( $m_R$ ).

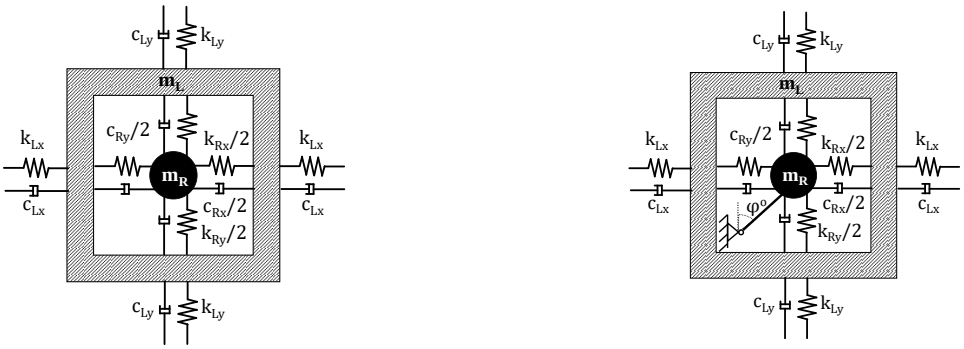


**Figure 2.** The periodic mass-in-mass unit-cell (a) w/o DDA (b) with DDA attached in the resonating mass ($m_R$)

When the units described above are arranged in a lattice structure with a distance of $L=\alpha_x=\alpha_y$, as shown in Figure 3, an infinitely periodic material is created. The lattice system is then analyzed for harmonic wave propagation in the mass-in-mass configuration.

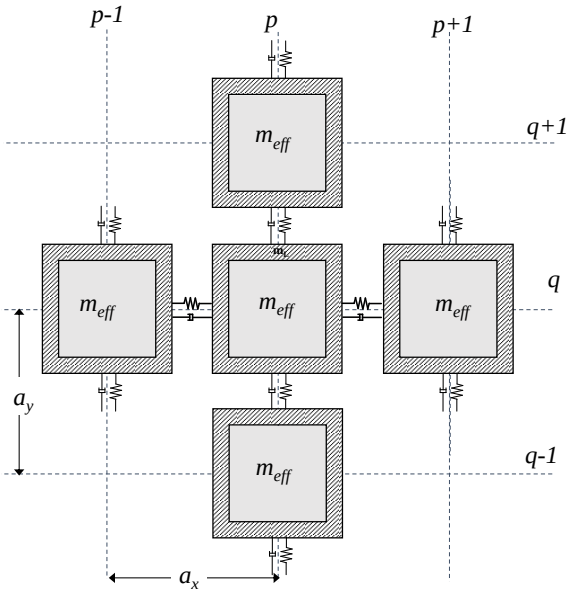


**Figure 3.** 2D spring-mass effective lattice.

Considering the case of the lattice under harmonic excitation, the relative motion of the structural nodes will cause amplified motion for the masses $m_R$ generating amplified inertial forces. Then, the wave propagation characteristics of this lattice are determined from the irreducible unit-cell via

Bloch's theorem. The dispersion relationship of the phononic structure with directional inertial amplifiers is given by:

$$\det[-\lambda^2 \boldsymbol{M}_{LRM-DDA} + \lambda \boldsymbol{C}_{LRM-DDA} \boldsymbol{K}_{LRM-DDA}] = 0 \tag{2}$$

where

$$\boldsymbol{M}_{LRM-DDA} = \boldsymbol{Q}^T \boldsymbol{M}_{LRM} \boldsymbol{Q} = \begin{bmatrix} m_L & 0 & 0 \\ 0 & m_L & 0 \\ 0 & 0 & m_R(1+\rho^2) \end{bmatrix}$$

$$\boldsymbol{C}_{LRM-DADA} = \boldsymbol{Q}^T \boldsymbol{C}_{LRM} \boldsymbol{Q} = \begin{bmatrix} 2c_{Lx}(1-\cos q_x) + c_{Rx} & 0 & -c_{Rx} \\ 0 & 2c_{Ly}(1-\cos q_y) + c_{R_y} & -\rho c_{R_y} \\ -c_{Rx} & -\rho c_{R_y} & c_{R_x}\rho^2 c_{R_y} \end{bmatrix} \tag{3}$$

$$\boldsymbol{K}_{LRM-DADA} = \boldsymbol{Q}^T \boldsymbol{K}_{LRM} \boldsymbol{Q} = \begin{bmatrix} 2k_{Lx}(1-\cos q_x) + k_{Rx} & 0 & -k_{Rx} \\ 0 & 2k_{Ly}(1-\cos q_y) + k_{R_y} & -\rho k_{R_y} \\ -k_{Rx} & -\rho k_{R_y} & k_{R_x}\rho^2 k_{R_y} \end{bmatrix}$$

## 3. Design of the Experimental Device

The conceptual configuration shown in Figure 4 includes an amplifier installed at the base of mass and is assembled using LEGO® Technic parts, except from the custom-made extension springs and the aluminium longitudinal guides. The use of LEGO® Technic parts was chosen due to its simplicity, cost-effectiveness, and accuracy compared to other alternatives such as steel structures or 3D printed elements. The design was first conceptualized and modeled in Lego Digital Designer to explore different arrangements before assembling the physical models. The structure consists of only three (3) unit-cells, which, according to previous studies can generate substantial bandgaps [20]. A hinged connection allows the link to rotate freely, and a fixed base supports the DDA mechanisms independently. The resonating mass ($m_R$) is connected to the external mass ($m_L$) using two extension springs.

The unit-cells are connected using an arrangement of springs [14], and to ensure proper functionality in both compression and extension, as depicted in Figure 5. The stable equilibrium position of the system is shifted backwards ($\Delta l$) by the compression spring, resulting in equivalent reactions in both the compression and extension states. This is in contrast to the original configuration, which is at its equilibrium position in full extension. This allows the system to react equivalently in both the compression and extension states, in contrast to the original configuration, which is at full extension at its equilibrium position. The overall stiffness of the assembly $k_n$ is therefore calculated as:

$$k_n = k_e + k_c \tag{4}$$

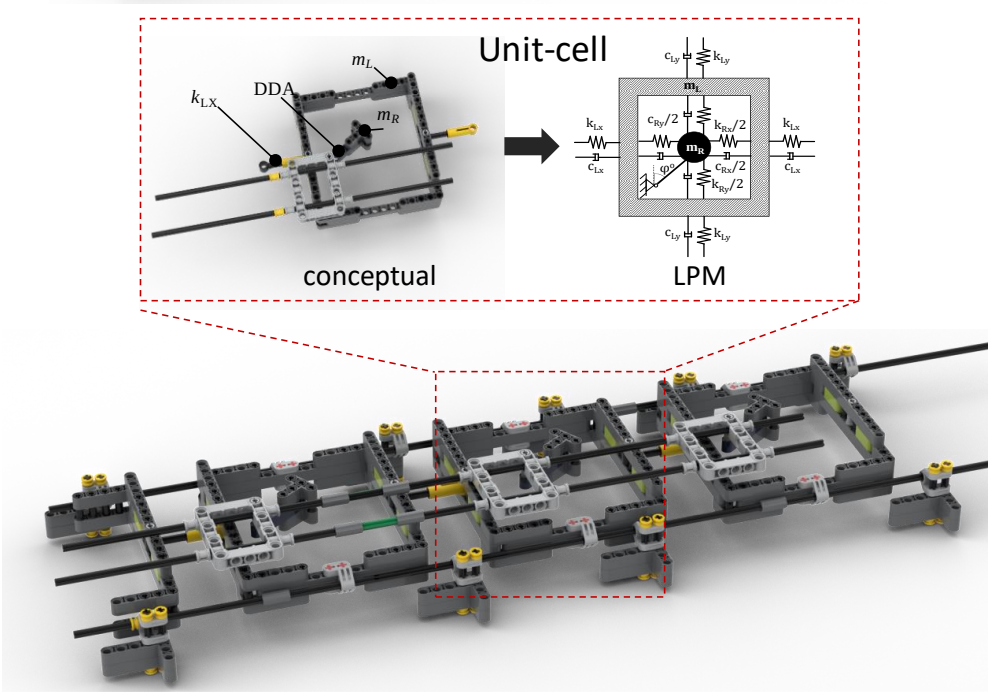


**Figure 4.** Illustration of the rendered LEGO® DDA enhanced locally resonant metamaterial design.

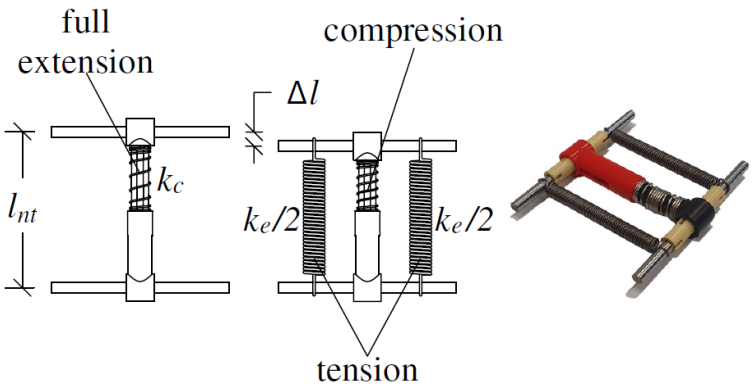


**Figure 5.** Assembly of the linear stiffness elements at rest: (left) original, (center) modified configuration, (right) physical assembly [14].

Table 1 presents an overview of the properties of the spring assemblies utilized in the models, including the stiffness value ( $k_n$ ), as well as the separate stiffness values of the extension spring ( $k_e$ ) and compression spring ( $k_c$ ).

**Table 1.** Stiffness characteristics of the experimentally tested springs.

| Extension spring $k_e$ [$Nm^{-1}$] | Compression spring $k_c$ [$Nm^{-1}$] | Spring Assembly $k_N$ [$Nm^{-1}$] |
|---|---|---|
| 80 | 320 | 480 |

The mass properties of the LR metamaterial structure are tabulated in Table 2. Mass $m_L$ is realized by LEGO ® parts, while mass $m_R$ is constructed by steel washers.

**Table 2.** Mass measurements for the individual parts of the experimental LR models.

| Element | Mass (g) |
|---|---|
| $m_L$ | 58 |
| $m_R$ | 58 |

## 4. Description of the Setup

The configured experimental setup is presented in Figure 6. An MB Modal 110 (MB Dynamics) electrodynamic shaker applies a one-dimensional (1D) horizontal input excitation. A timber board is mounted at the shaker's shaft on one side, to function as a shaking table, while longitudinal guides and bearings provide support, maintain the table in a levelled position, and limit parasitic vertical oscillations. A digital signal generator creates the harmonic sweep and a 2050E05 (modal shop INC) amplifier receives the produced signal and activates the shaker. Both sinusoidal inputs as well as sine sweeps can be generated by controlling the voltage signal of the shaker. This signal results to a nearly flat spectrum for a given frequency range, thus exciting uniformly the specified range.

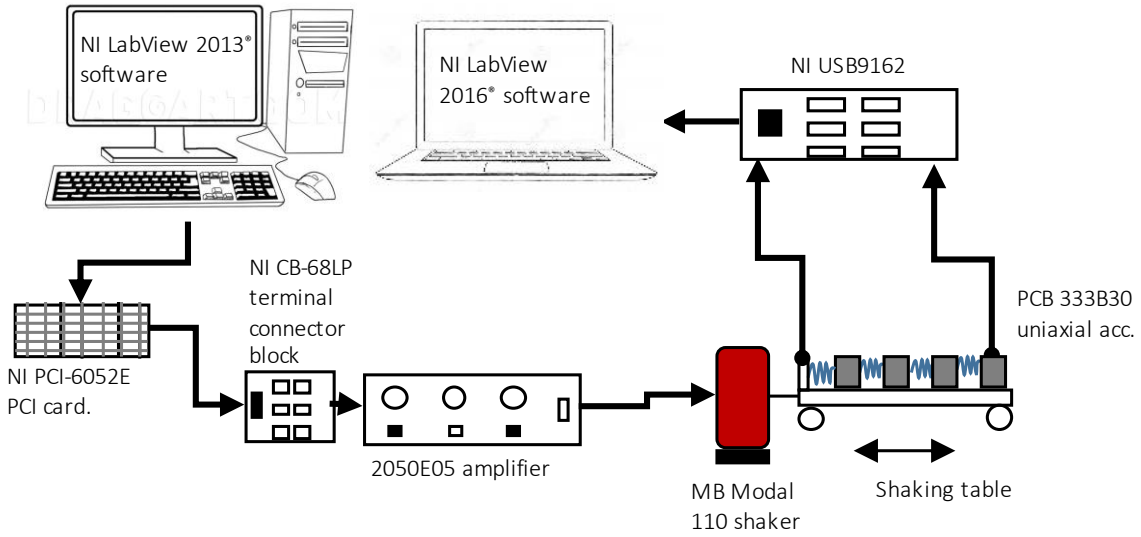


**Figure 6.** Schematic diagram of the experimental setup.

The metamaterial chain is positioned on the shaking table, with longitudinal guides ensuring that movements occur primarily in the intended direction. To minimize friction between the guides and the support, a lubricant liquid is used, although some minimal friction is still present. The cells are entirely disconnected from the shaking table except for the support of the first cell, which is mounted to the table's shaker to create longitudinal wave propagation within the lattice.

The system's dynamic response is measured using uniaxial PCB 333B30 accelerometers, which have a sensitivity of 10.2 mV/m/s² and a sampling frequency of 2 kHz. The measurements are taken at various locations, including the last unit-cell and the shaker input signal. An NI USB9162 card is used

to connect the accelerometers to the computer, and data recording is performed through the NI LabView 2016® software. In-house scripts developed on MATLAB R2020b® software are used for post-processing the data.

The DDA enhanced lattice is presented in Figure 7. The design is centered around a mass-in-mass configuration where the resonating mass is linked to the external mass through two extension springs. A LEGO® assembly supports the amplifiers above the shaking table providing a steady ground to the hinged connections. The Amplifier's angle is selected as $\varphi \approx 55°$.

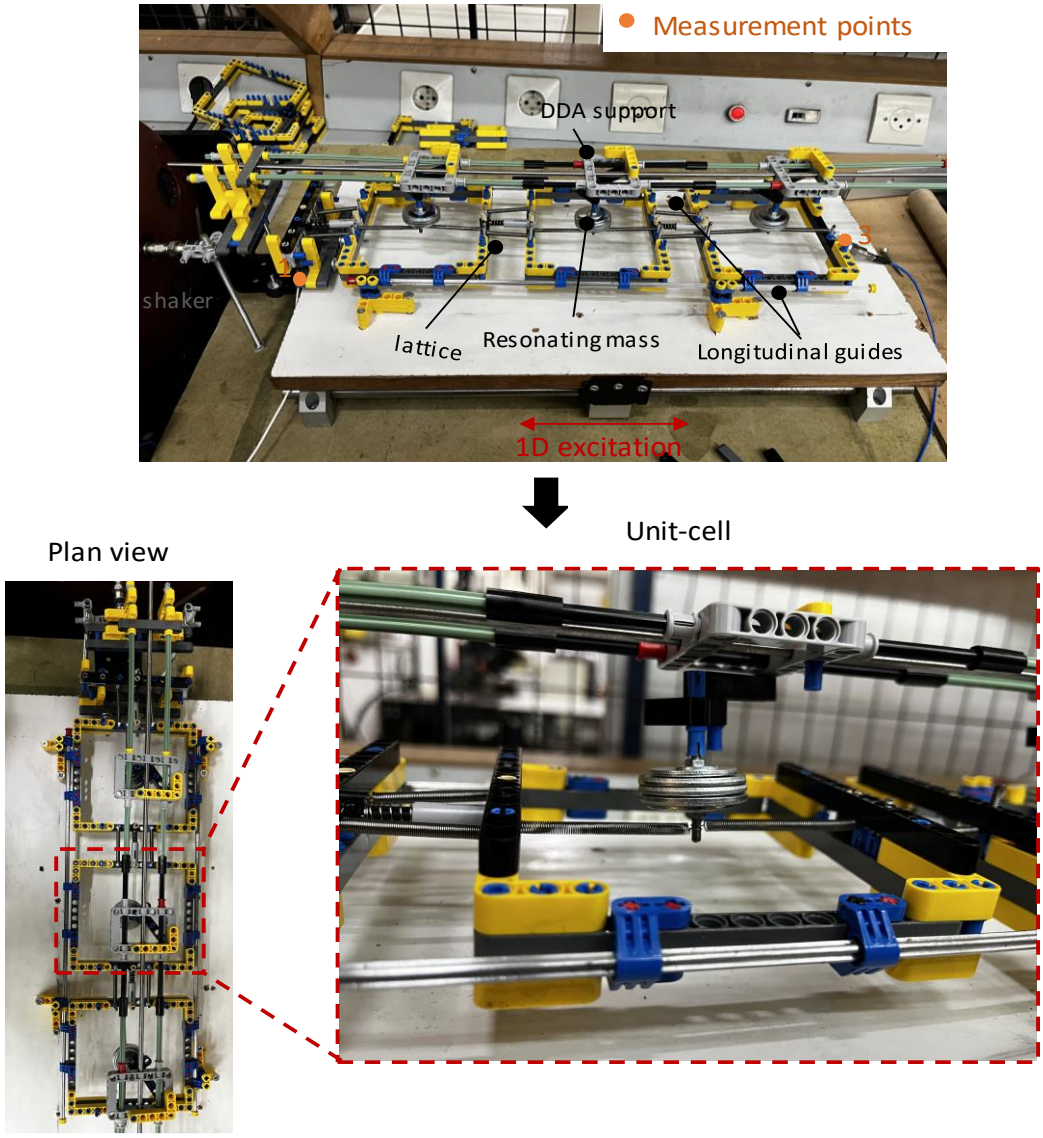


Figure 7: Overview of the LEGO® DDA enhanced Locally resonant (LR) structure comprised of three (3) unit-cells.

## 5. Experimental Results

This section examines the obtained experimental results. Both sine-sweep and single-harmonic inputs were used in the tests, with acceleration measurements carried out using small amplitude excitations to ensure the linear elastic behaviour of the metamaterial. The wave transmission spectrum is obtained by

calculating the ratio of output to input spectral accelerations $F\left\{\ddot{u}_{fin}^{out} / \ddot{u}_{1}^{in}\right\}$, using the FFT function. The attenuation capabilities of each metamaterial device is evaluated based on this spectrum, and the efficiency of each device is assessed by comparing its attenuation zone to the analytically predicted bandgaps.

The analysis of the experimental results of the LR structures begins with the theoretical estimation of the dispersion curves. Figure 8 (a) indicates the frequency range that an attenuation zone is expected from the experimental measurements before and after the addition of the amplifiers. The conventional structure is expected to present an attenuation zone between 7.1 and 10.1 Hz and this zone is expected to be increased by 113% after the inclusion of the DDAs. Thus, in order to validate the design of the locally resonant structure before progressing with the enhanced lattice, the experimentally measured dynamic response of the metamaterial is compared with the analytically estimated frequency response, provided in Figure 8 (b). Indeed, the two curves are in agreement, bearing in mind all the potential discrepancies and especially the role of friction among the units and the guides. A certain amount of damping, in the form of damping ratio ($\zeta = 7\%$) is assumed in the theoretical model, originating from the guides-units friction, aiming to fit the experimental curve.

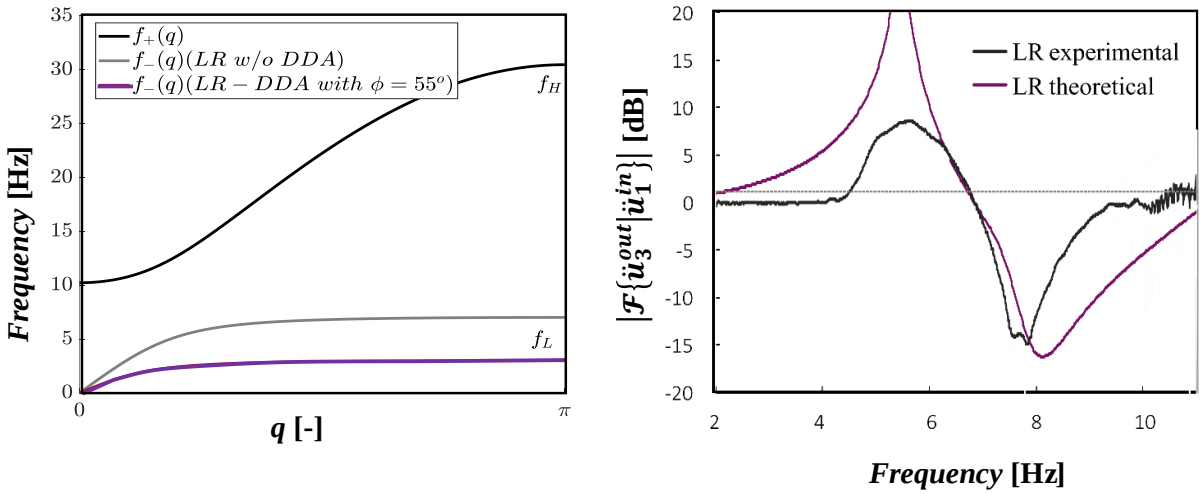


(a) (b)

**Figure 8.** (a) Expected theoretical dispersion curves of the LR LEGO® Technic assemblies. (b) Comparison between the experimental and analytically estimated frequency response $F\{\ddot{u}_4^{out}|\ddot{u}_1^{in}\}F\{\ddot{u}_4^{out}|\ddot{u}_1^{in}\}F\{\ddot{u}_4^{out}|\ddot{u}_1^{in}\}$ for the four (3) unit-cell chain of the LR structure.

Figure 9 illustrates the frequency response of the conventional and enhanced LR metamaterial device, as measured experimentally. The size of the attenuation zones is used to evaluate the response of the two metamaterials. The "conventional" locally resonant structure exhibits a bandgap ranging from 7.5 to 10.1 Hz, which aligns with the theoretical estimation. On the other hand, the DDA-enhanced structure demonstrates a bandgap between 4.5 and 9.5 Hz, which is slightly smaller than the theoretical estimations (indicated by shaded areas). Overall, the dynamic response of the proposed prototypes verifies the analytically predicted response of the two arrangements, exhibiting the capabilities of the DDA enhanced LR lattices.

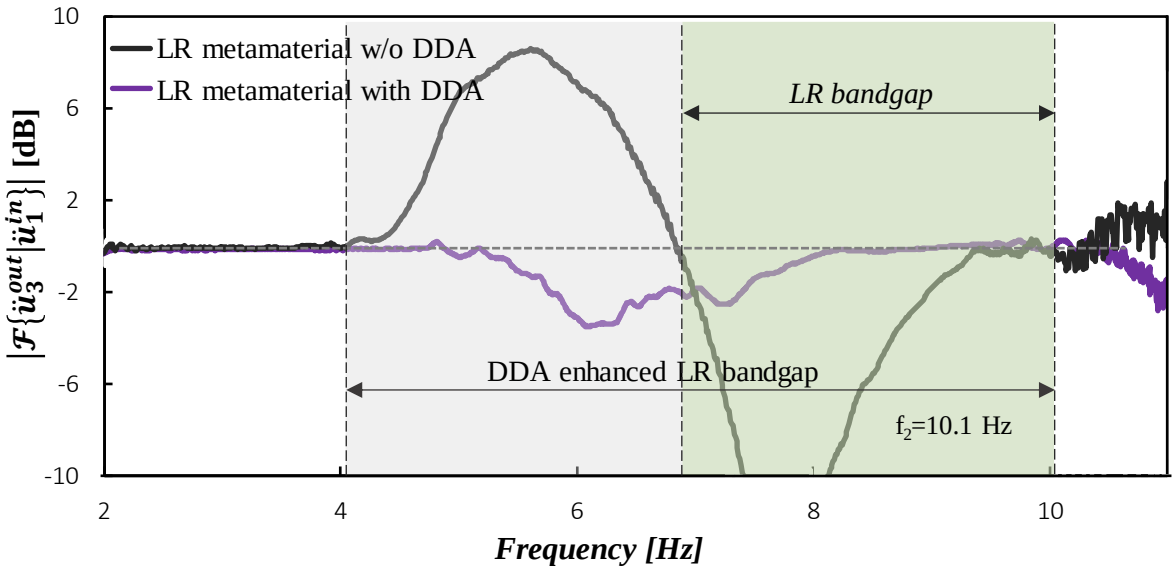


**Figure 9.** Frequency content of the response of the LR lattice with and w/o the DDA ($\varphi$=55°) for a three (3) unit-cell lattice. The maximum acceleration of each unit $p$ is denoted as max $\ddot{u}_p^L$.

## 6. CONCLUSIONS

This work experimentally investigates the dynamics and filtering properties of DDA-enhanced LR periodic structures through experimental methods. The unit-cells of the lattices are composed of LEGO® assemblies connected through spring assemblies comprised of compression and extension springs. The experimental transmission spectrum of the finite-sized locally resonant structure exhibits a substantial signal reduction within the identified bandgap region initially determined by the dispersion analysis, when only three (3) unit cells are considered. Incorporating the DDA mechanism further enhances the metamaterial's behaviour, extending the attenuation zone to lower frequencies, while reducing the bandgap depth and mitigating the resonant peaks outside the attenuation zone. The conclusion is that the DDA inertial amplification mechanism can improve the design of vibration mitigation and shock-absorbing metamaterials at various length scales. While this is an initial investigation, validated by a scaled proof-of-concept system, further study is necessary to determine the feasibility of the proposed designs and potential practical limitations prior to proceeding to realistic full-scale applications. The practical implementation aspects of the proposed designs for seismic protection of structures, energy harvesting, or acoustic absorption are topics of interest for future examination.

**Acknowledgments**

M. Kalderon, A. Mantakas & K.A. Chondrogiannis would like to acknowledge the financial support provided by the European Union's Horizon 2020 research and innovation program under the Marie Sklodowska-Curie grant (Grant Agreement No. INSPIRE-813424).

**References**

[1] J. Li, C.T. Chan, Double-negative acoustic metamaterial, Phys. Rev. E. 70 (2004) 55602. https://doi.org/10.1103/PhysRevE.70.055602.

[2] Y. Ding, Z. Liu, C. Qiu, J. Shi, Metamaterial with Simultaneously Negative Bulk Modulus and Mass Density, Phys. Rev. Lett. 99 (2007) 93904. https://doi.org/10.1103/PhysRevLett.99.093904.

[3] M.I. Hussein, M.J. Frazier, Band structure of phononic crystals with general damping, J. Appl. Phys. 108 (2010) 93506. https://doi.org/10.1063/1.3498806.

[4] H.H. Huang, C.T. Sun, G.L. Huang, On the negative effective mass density in acoustic metamaterials, Int. J. Eng. Sci. 47 (2009) 610–617. https://doi.org/https://doi.org/10.1016/j.ijengsci.2008.12.007.
[5] P.P. Kulkarni, J.M. Manimala, Longitudinal elastic wave propagation characteristics of inertant acoustic metamaterials, J. Appl. Phys. 119 (2016) 245101. https://doi.org/10.1063/1.4954074.
[6] G. Liao, C. Luan, Z. Wang, J. Liu, X. Yao, J. Fu, Acoustic Metamaterials: A Review of Theories, Structures, Fabrication Approaches, and Applications, Adv. Mater. Technol. 6 (2021) 1–29. https://doi.org/10.1002/admt.202000787.
[7] Y. Zeng, L. Cao, S. Wan, T. Guo, Y.-F. Wang, Q.-J. Du, B. Assouar, Y.-S. Wang, Seismic metamaterials: Generating low-frequency bandgaps induced by inertial amplification, Int. J. Mech. Sci. 221 (2022) 107224. https://doi.org/10.1016/j.ijmecsci.2022.107224.
[8] S. Muhammad, S. Wang, F. Li, C. Zhang, Bandgap enhancement of periodic nonuniform metamaterial beams with inertial amplification mechanisms, J. Vib. Control. 26 (2020) 1309–1318. https://doi.org/10.1177/1077546319895630.
[9] M. Mazzotti, A. Foehr, O.R. Bilal, A. Bergamini, F. Bosia, C. Daraio, N.M. Pugno, M. Miniaci, Bio-inspired non self-similar hierarchical elastic metamaterials, Int. J. Mech. Sci. 241 (2023) 107915. https://doi.org/10.1016/j.ijmecsci.2022.107915.
[10] A. Paradeisiotis, M. Kalderon, I. Antoniadis, Advanced negative stiffness absorber for low-frequency noise insulation of panels, AIP Adv. 11 (2021) 65003. https://doi.org/10.1063/5.0045937.
[11] S. Taniker, C. Yilmaz, Generating ultra wide vibration stop bands by a novel inertial amplification mechanism topology with flexure hinges, Int. J. Solids Struct. 106–107 (2017) 129–138. https://doi.org/10.1016/j.ijsolstr.2016.11.026.
[12] S. Taniker, C. Yilmaz, Design, analysis and experimental investigation of three-dimensional structures with inertial amplification induced vibration stop bands, Int. J. Solids Struct. 72 (2015) 88–97. https://doi.org/10.1016/j.ijsolstr.2015.07.013.
[13] R. Zaccherini, A. Colombi, A. Palermo, H.R. Thomsen, E.N. Chatzi, Stress-optimized inertial amplified metastructure with opposite chirality for vibration attenuation, (2021). https://doi.org/https://doi.org/10.48550/arXiv.2111.08594.
[14] K.A. Chondrogiannis, A. Colombi, V. Dertimanis, E. Chatzi, Computational Verification and Experimental Validation of the Vibration-Attenuation Properties of a Geometrically Nonlinear Metamaterial Design, Phys. Rev. Appl. 17 (2022) 54023. https://doi.org/10.1103/PhysRevApplied.17.054023.
[15] M. Kalderon, A. Paradeisiotis, I. Antoniadis, 2D Dynamic Directional Amplification (DDA) in Phononic Metamaterials, Materials (Basel). 14 (2021). https://doi.org/10.3390/ma14092302.
[16] M. Kalderon, A. Paradeisiotis, I.A. Antoniadis, A Phononic Metamaterial Incorporating Directional Amplification for Low Frequency Isolation, in: Proc. Int. Conf. Nat. Hazards Infrastruct., 2022.
[17] X. An, C. Lai, W. He, H. Fan, Three-dimensional meta-truss lattice composite structures with vibration isolation performance, Extrem. Mech. Lett. 33 (2019) 100577. https://doi.org/10.1016/j.eml.2019.100577.
[18] Q. Lin, J. Zhou, H. Pan, D. Xu, G. Wen, Numerical and Experimental Investigations on Tunable Low-frequency Locally Resonant Metamaterials, Acta Mech. Solida Sin. 34 (2021) 612–623. https://doi.org/10.1007/s10338-021-00220-4.
[19] M. Kalderon, A. Mantakas, I. Antoniadis, Dynamic Modelling and Experimental Testing of a Dynamic Directional Amplification Mechanism for Vibration Mitigation, J. Vib. Eng. Technol. (2023). https://doi.org/10.1007/s42417-023-00925-5.
[20] P. Martakis, G. Aguzzi, V.K. Dertimanis, E.N. Chatzi, A. Colombi, Nonlinear periodic foundations for seismic protection: Practical design, realistic evaluation and stability considerations, Soil Dyn. Earthq. Eng. 150 (2021) 106934. https://doi.org/10.1016/j.soildyn.2021.106934.